Received: 27 November 2020 | Revised: 4 January 2021 | Accepted: 5 January 2021

DOI: 10.1111/gtc.12828

ORIGINAL ARTICLE

Genes to Cells WILEY

TET3 dioxygenase modulates gene conversion at the avian immunoglobulin variable region via demethylation of non-CpG sites in pseudogene templates

Natsuki Takamura[1] | **Hidetaka Seo**[1] | **Kunihiro Ohta**[1,2]

[1]Department of Life Sciences, Graduate School of Arts and Sciences, The University of Tokyo, Meguro-ku, Japan

[2]Universal Biology Institute, The University of Tokyo, Bunkyo-ku, Japan

Correspondence
Kunihiro Ohta, Department of Life Sciences, Graduate School of Arts and Sciences, The University of Tokyo, Komaba 3-8-1, Meguro-ku, Tokyo 153-8902, Japan
Email: kohta-pub2@bio.c.u-tokyo.ac.jp

Funding information
Grant-in-Aid for Basic Science, Grant/Award Number: 20K06598; JST CREST, Grant/Award Number: JPMJCR18S3

Communicated by: Takehiko Kobayashi

Abstract

Diversification of the avian primary immunoglobulin (Ig) repertoire is achieved in developing B cells by somatic hypermutation (SHM) and gene conversion (GCV). GCV is a type of homologous recombination that unidirectionally transfers segments of Ig pseudogenes to Ig variable domains. It is regulated by epigenetic mechanisms like histone modifications, but the role of DNA methylation remains unclear. Here, we demonstrate that the chicken B-cell line DT40 lacking TET3, a member of the TET (Ten-eleven translocation) family dioxygenases that facilitate DNA demethylation, exhibited a marked reduction in GCV activity in Ig variable regions. This was accompanied by a drop in the bulk levels of 5-hydroxymethylcytosine, an oxidized derivative of 5-methylcytosine, whereas TET1-deficient or TET2-deficient DT40 strains did not exhibit such effects. Deletion of TET3 caused little effects on the expression of proteins required for SHM and GCV, but induced hypermethylation in some Ig pseudogene templates. Notably, the enhanced methylation occurred preferably on non-CpG cytosines. Disruption of both TET1 and TET3 significantly inhibited the expression of activation-induced cytidine deaminase (AID), an essential player in Ig diversification. These results uncover unique roles of TET proteins in avian Ig diversification, highlighting the potential importance of TET3 in maintaining hypomethylation In Ig pseudogenes.

KEYWORDS

DNA demethylation, gene conversion, immunoglobulin, non-CpG methylation, pseudogene, TET protein

1 | INTRODUCTION

DNA methylation is one of the major mechanisms of epigenetic regulation, as it constitutes a heritable cellular memory independently of changes in the genome's nucleotide sequence (Bird, 2002; Suzuki & Bird, 2008). DNA methylation is frequently involved in the regulation of chromosomal functions such as gene expression, DNA repair and recombination (Cedar & Bergman, 2009; Esteller, 2007; Jaenisch & Bird, 2003; Robertson & Wolffe, 2000; Schlissel, 2004). It is introduced by DNA methyltransferases (DNMTs) that catalyze the covalent modification of a methyl group to cytosine to form 5-methylcytosine (5mC) (Goll & Bestor, 2005). In mammals,

most of DNA methylation occurs in a CpG context in many differentiated somatic cells, although it can also occur at cytosines in a non-CpG context in some cell types, including embryonic stem (ES) cells, induced pluripotent stem (iPS) cells, neurons and glial cells (Jang et al., 2017; Lister et al., 2009; Ziller et al., 2011). DNA methylation in a non-CpG context is much more frequently observed in plant genomes (Feng et al., 2010; Lindroth et al., 2001). CpG methylation in promoter regions often leads to the establishment of repressive histone modifications and the formation of heterochromatin regions, where gene expression is severely repressed (Cedar & Bergman, 2009). On the other hand, the hypermethylation of CpG sites within the gene body is associated with increased expression (Lister et al., 2009; Yang et al., 2014). Although non-CpG methylation has been reported for decades, their functions remain elusive (Jang et al., 2017; Patil et al., 2014).

DNA methylation status is determined by the balance between DNA methylation and demethylation reactions. DNA demethylation can occur either passively through DNA replication or actively through the action of a dioxygenase family known as "Ten-eleven translocation proteins" (TET proteins), including TET1, TET2 and TET3 in mammalian cells (Pastor et al., 2013; Wu & Zhang, 2017). They successively oxidize 5mC to 5-hydroxymethylcytosine (5hmC), 5-formylcytosine (5fC) and finally 5-carboxylcytosine (5caC), which are then removed by thymine DNA glycosylase (TDG). The resulting apurinic/apyrimidinic (AP) site is restored by an unmodified cytosine through base excision repair (BER), thereby completing active demethylation of 5mC (He et al., 2011; Ito et al., 2011; Weber et al., 2016). TET proteins contain a cysteine-rich domain and a double-stranded β-helix (DSBH) domain, which coordinates Fe(II) and interacts with 2-oxoglutarate (2-OG) as cofactors (Figure 1a; DSBH domains are represented as catalytic domain (CD) 1 and 2) (Hu et al., 2013; Pastor et al., 2013). In addition, mammalian TET1 and TET3 harbor a CXXC zinc finger domain that can bind DNA (Xu et al., 2011, 2012). TET proteins are reportedly important in the maintenance of cell pluripotency, differentiation, neuronal functions and cancer development (Rasmussen & Helin, 2016; Wu & Zhang, 2017). For example, the *TET2* gene is frequently mutated in hematopoietic malignancies, and its dysfunction is sometimes accompanied with the onset of cancer (Delhommeau et al., 2009; Weissmann et al., 2012).

Diversity of the B-cell receptor (antibody) is established by several mechanisms: V(D)J recombination, but also somatic hypermutation (SHM), class switch recombination and gene conversion (GCV) events. In avian B cells, V(D)J recombination contributes little to the primary diversification of the variable regions for heavy chain (HC) and light chain (LC), whereas GCV, a type of unidirectional homologous recombination (HR), largely plays a major role in the generation of primary repertoire (Ratcliffe, 2006; Reynaud et al., 1985, 1989). GCV utilizes recombination donor templates of immunoglobulin (Ig) pseudogenes located in the near upstream region of the V(D)J recombined active Ig loci, as they show similarity to the functional V region (Ratcliffe, 2006; Reynaud et al., 1987).

It should be noted that non-V(D)J recombination antibody diversification processes require a central APOBEC-family enzyme known as activation-induced cytidine deaminase (AID) (Arakawa et al., 2002; Muramatsu et al., 2000). Various AID-dependent Ig diversification pathways are thought to be triggered by the occurrence of DNA lesions (single strand nicks or double strand breaks) followed by the removal of the AID-deaminated deoxycytidine (i.e., deoxyuracil) either by BER (removal of a uridine by Uracil-DNA glycosylase followed by AP endonuclease which introduces a DNA nick) or by mismatch repair (MMR: repair by mismatch recognition, followed by excision and replacement of the incorrect strand) (Di Noia & Neuberger, 2007). However, the molecular mechanism for the initial event of AID to induce Ig diversification still needs to be more extensively elucidated.

DT40 is a chicken-derived B-cell line where GCV is continuously occurring at the active Ig variable region (Baba et al., 1985; Buerstedde et al., 1990). We previously reported that the frequency of GCV (and SHM) in DT40 is markedly enhanced when DT40 is cultured in a medium containing a histone deacetylase inhibitor trichostatin A (TSA) (Seo

FIGURE 1 Construction of *TET1*-KO, *TET2*-KO and *TET3*-KO DT40 cell lines and the effects on transcription of *DNMT1*, *DNMT3A*, *IgVλ* and *AID* genes. (a) Schematic diagrams of chicken TET1, TET2 and TET3 proteins with DSBH domains (denoted as CD1 and CD2: catalytic domain 1 and 2). The insertion sites of disruption markers to the genomic loci are indicated. Numbers are the position of amino acid residues. "aa" represents amino acids. (b) Principle of the sIgM gain assay. The CL18 strain harbors a frameshift in its *IgVλ* locus, resulting in a sIgM(−) phenotype. The mutation is restored predominantly by GCV (very rarely by SHM) thereby generating sIgM(+) cells. Thus, the reversion rate from sIgM(−) to sIgM(+) almost exclusively reflects the frequency of Ig GCV events. (c) *DNMTs* mRNA levels in WT, *TET1*-, *TET2*- and *TET3*-KO cells quantified by RT-qPCR. The expression levels were normalized to β-actin and then to the WT levels. The thin vertical bars demonstrate the standard deviation (*SD*) of four biological replicates. The *p*-values were calculated with unpaired *t* test with Welch's correction (ns; not statistically significant, $*p < .05$, $**p < .01$, $***p < .001$, $****p < .0001$). (d) *IgVλ* mRNA levels in WT and all single *TET* mutants quantified by RT-qPCR. The expression levels were normalized as described in (c). The error bars show the *SD* of at least six biological replicates (from left to right: $n = 20$, $n = 6$, $n = 9$ and $n = 6$). The *p*-values were as described above. (e) *AID* mRNA levels in WT and all single *TET* mutants quantified by RT-qPCR. The expression levels were analyzed and shown as described in (c) and (d) (from left to right: $n = 4$, $n = 12$, $n = 16$ and $n = 19$)

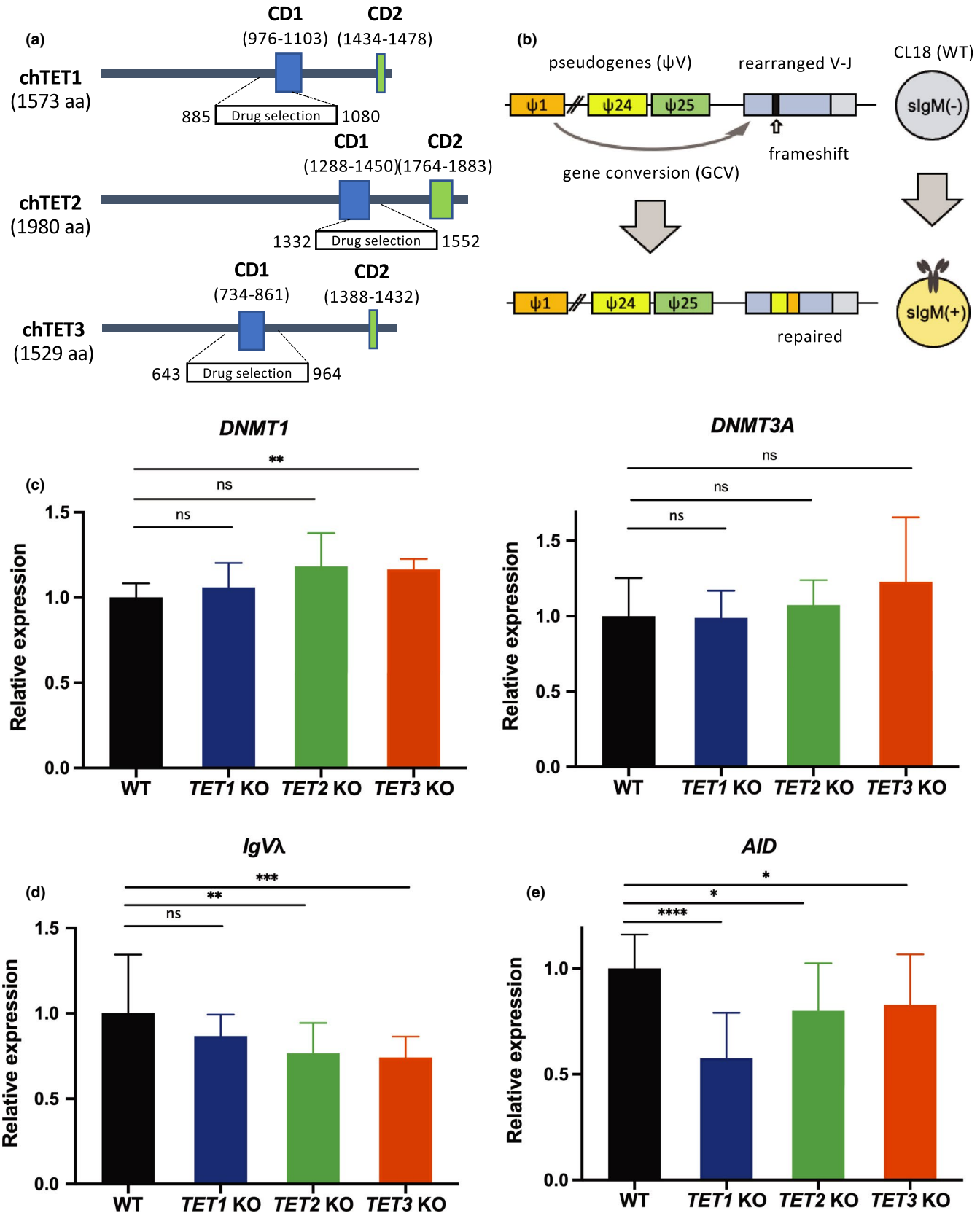

et al., 2005, 2006). This higher frequency of GCV is concomitant with the increase in histone acetylation levels around the Ig variable region and the corresponding induction of IgLC transcription, indicating that TSA-mediated formation of accessible chromatin configuration can promote GCV. In addition, our subsequent studies showed histone deacetylase

HDAC1 and HDAC2 modulate GCV in DT40 cells (Kurosawa et al., 2010; Lin et al., 2008). These results suggest that local epigenetic configuration influences the GCV and SHM frequency. However, little is known about the contribution of local DNA methylation to the regulation of Ig diversification.

Here, we investigated the role of TET proteins in Ig diversification using DT40 and demonstrated that DT40 lacking TET3 exhibited a marked reduction in GCV activity in Ig variable regions, concomitant with a drop in the bulk levels of 5hmC and the local increase in 5mC at non-CpG cytosines in Ig pseudogene segments. Although *TET3*-KO only had a slight effect on the expression of proteins required for SHM and GCV such as AID, the double KO of *TET1* and *TET3* resulted in severe AID deficiency. These results suggest that TET3 plays a critical role in avian Ig diversification *via* the modulation of non-CpG methylation in Ig pseudogenes.

2 | RESULTS

2.1 | Effects of single knockouts for *TET1*, *TET2* and *TET3* genes on cell growth and gene expression in chicken B-cell line DT40

To examine the roles of TET proteins in Ig diversification, we conducted homologous gene targeting to establish single knockout (KO) mutants for *TET1*, *TET2* and *TET3* genes (*TET1*-KO, *TET2*-KO and *TET3*-KO, respectively) in a DT40-derived line "Clone 18 (CL18)", which harbors a frameshift in the rearranged Ig light chain variable (*IgVλ*) segment. The CL18 strain thus exhibits a surface IgM negative (sIgM(−)) phenotype (Buerstedde et al., 1990), while it is converted to a surface IgM positive (sIgM(+)) when the frameshift mutation is restored by gene conversion (GCV) events using intact pseudogene segments as recombination templates (Figure 1b).

Deletions of the *TET* genes were targeted to their DSBH domain, which has been implicated in Fe(II)/2-OG dependent dioxygenase activity catalyzing an oxidation reaction into its substrate (Figure 1a; DSBH domains are shown as CD1 and 2). The deletions were confirmed by genomic PCR (Figure S1a). The disruption of each *TET* gene was also confirmed by loss of mRNA expression quantified with RT-qPCR experiments (Figure S1b).

We then examined the effects of *TET* gene single deletions on cell proliferation (Figure S1c). The cell growth speed and doubling time of each *TET* KO strain were almost identical to those of the *TET*-intact wild-type (WT) CL18 cells. Thus, we concluded that cell proliferation of DT40 is not significantly affected by any single KO deletion of *TET* genes.

Next, we assessed the influence of each single *TET* KO mutant on the expression of DNA methyltransferases (DNMTs, DNMT1 and DNMT3A) (Figure 1c), since methylation levels are established *via* the competing enzymatic activities of DNMTs and TET proteins (Ginno et al., 2020; Ravichandran et al., 2018; Verma et al., 2018). We observed a faint but statistically significant increase in the expression of *DNMT1* in *TET3*-KO cells (1.17-fold). All in all, single *TET* KO mutants seem to have a very limited effect on the expression of *DNMT1,* and no effects on *DNMT3A* (Figure 1c).

We also examined the expression levels of active *IgVλ* (Figure 1d) and *AID* (an essential player in Ig diversification) (Figure 1e). The effects of single *TET* KOs on the expression of *IgVλ* were similarly slight, with *TET2*-KO and *TET3*-KO exhibiting a 25% reduction in *IgVλ* expression (Figure 1d). On the other hand, *AID* expression levels were moderately reduced in *TET1*-KO (to about 40% of the WT level), but less so in *TET2*-KO and *TET3*-KO cells (by about 20%) (Figure 1e). We further examined other genes (*CTNNBL1*, *BACH2*, *FANCD2*, *DDX11*, *PARP1*, *POLH* and *RNF8*) (Abe et al., 2018) for Ig GCV in *TET3*-KO (Figure S2), since *TET3*-KO exhibited marked deficiency in Ig GCV (see below). We did not observe any significant variation of the expression levels of these factors for Ig GCV. In general, it can be concluded that single *TET* KO mutants had a limited impact on the expression of Ig gene diversification factors.

2.2 | Disruption of TET3 reduces diversification of *IgVλ* in DT40 cells

To determine whether TET proteins are involved in the Ig diversification, we studied *TET1*-KO, *TET2*-KO and *TET3*-KO strains using the surface IgM (sIgM) gain assay. This assay measures the reversion from sIgM(−) to sIgM(+) phenotype through the repair of the CL18-type frameshift, which is almost exclusively attributable to GCV events around the frameshift mutation (Arakawa et al., 2002; Buerstedde et al., 1990) (Figure 1b). The sIgM(−) CL18 subclones from WT and each *TET*-deficient mutant were first cloned by limiting dilution and the frequency of sIgM(+) population of individual subclones was determined by flow cytometry. After about 1 month of clonal expansion, we observed that frequency of conversion to sIgM(+) was significantly lower than that of WT in all *TET*-deficient mutants, with *TET3* KO cells being the most severely affected (Figure 2a).

This tendency was also observed in the subclones cultured in medium supplemented with TSA, a histone deacetylase inhibitor that promotes chromatin accessibility and enhances the Ig GCV (Seo et al., 2005, 2006) (Figure 2b). In TSA-treated conditions, *TET3*-KO cells showed a much greater reduction of *IgVλ* GCV than either *TET1*-KO or *TET2*-KO cells, suggesting the importance of TET3 in Ig diversification independently of TSA-induced local chromatin configuration changes.

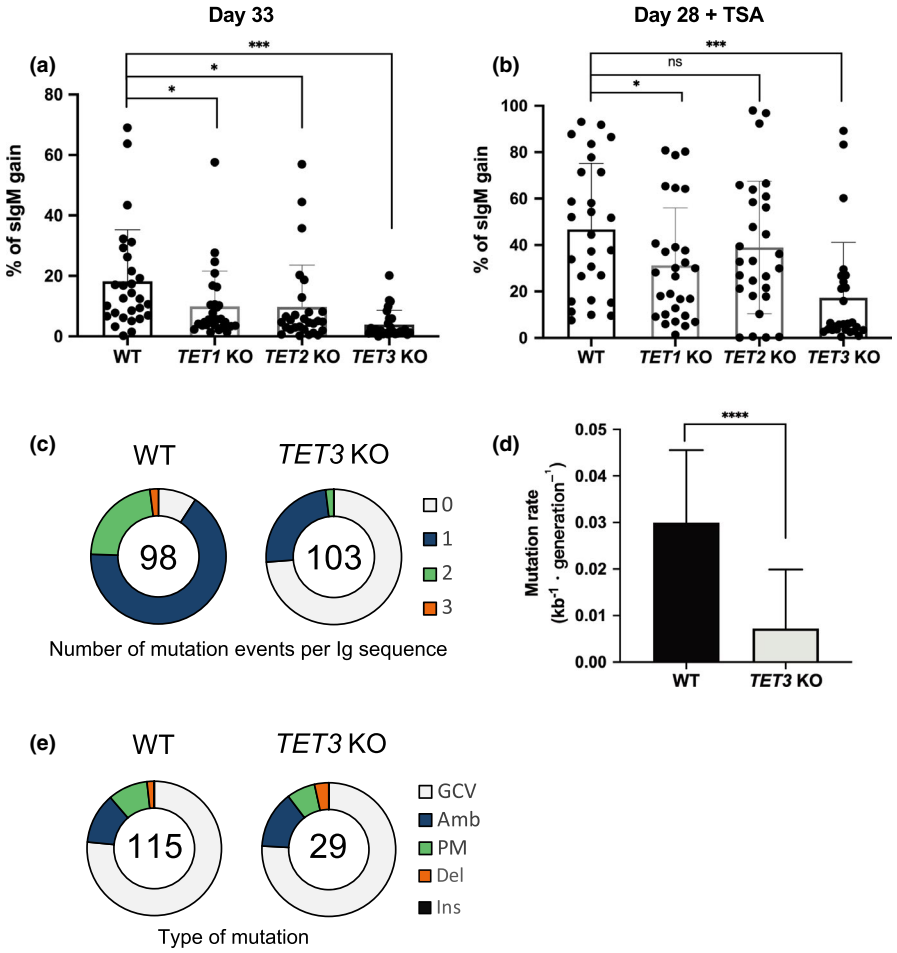

FIGURE 2 Reduced diversification of the Ig light chain variable region (*IgVλ*) in *TET3*-KO cells. (a) The sIgM gain assay of WT, *TET1*-KO, *TET2*-KO and *TET3*-KO DT40 cells without TSA treatment. The percentage of sIgM(+) cells was determined by flow cytometry after 33 days of culture. A total of 27–28 subclones (represented by circles) per cell line were analyzed. The thin vertical bars are the *SD* of all subclones. The *p*-values were calculated with the unpaired *t* test with Welch's correction (ns; not statistically significant ($p > .05$), *$p < .05$, ***$p < .001$). (b) The sIgM gain assay after 28 days of culture with TSA treatment. Data were obtained and analyzed as described in (a). (c) Frequency of mutations occurred in *IgVλ* in WT and *TET3*-KO cells. The total number of the examined sequences is indicated in the center of each chart. (d) Mutation rate per kilobase per generation in WT and *TET3*-KO cells. The frequencies of mutation events were calculated from sequences analyzed in (c). The number of generations is based on the growth curve of each cell line (Figure S1c). The thin vertical bars show the *SD* of all sequences analyzed (****$p < .0001$, unpaired *t* test with Welch's correction). (e) Spectrum of Ig sequence diversification in WT and *TET3*-KO cells. Mutations are classified as described in Experimental procedures. The number of total mutations is indicated in the center of each chart. GCV; gene conversion, Amb; ambiguous, PM; point mutation, Del; deletion, Ins; insertion

We then clarified the exact magnitude and spectrum of sequence alterations by sequencing the rearranged *IgVλ* of WT and *TET3*-KO cells after a 4-week culture (Figure 2c–e). Consistent with the results of the sIgM gain assay, only 26% of the *TET3*-KO population had single or double sequence alterations, while 91% of the WT demonstrated single, double, or triple sequence alterations (Figure 2c). Moreover, the mutation rate was reduced in *TET3*-KO cells to 24% of the WT level (Figure 2d).

Despite the difference in frequency, WT and *TET3*-KO cells exhibited a very similar spectrum of sequence alterations (Figure 2e). As observed in WT DT40 and natural chicken B cells (McCormack et al., 1991; Reynaud et al., 1987), Ig diversification in *TET3*-KO DT40 largely relied upon GCV. Previous studies have shown that genes involved in Ig diversification control the different steps of GCV and/or SHM (Abe, Branzei, et al., 2018). The disruption of genes for HR, such as *XRCC2/3* (Sale et al., 2001), severely impairs GCV while increasing the frequency of SHM. On the other hand, the genes required for the induction of mutations, such as *AID* and *BACH2* (Arakawa et al., 2002; Budzyńska et al., 2017), and the genes involved in the selection of repair pathway, including *PARP1* (Paddock et al., 2010), are needed to sustain both GCV and SHM. Considering these reports and the unaltered spectrum in *TET3*-KO cells, TET3 is dispensable for the GCV process per se but may be important in the initiation

or template selection of GCV. This idea is consistent with the results that *TET3* deletion did not influence the expression of genes involved in GCV (see Figure S2).

As another possible mechanism for the GCV deficiency in *TET3*-KO cells, we do not completely rule out the possibility that HR process itself could be impaired by the disruption of *TET3* gene. However, this is unlikely, since multiple reports have indicated that HR-deficient mutants often exhibit cell growth retardation (Abe, Ooka, et al., 2018; Oestergaard et al., 2012; Yamamoto et al., 2005), whereas *TET3*-KO strain does not (Figure S1c). Taken together with the unaltered mutation spectrum in *TET3*-KO cells (Figure 2e), these results again suggest that TET3 targets earlier stages than the HR reaction process.

2.3 | Absence of TET3 leads to altered usage of pseudogene templates for GCV

We further investigated the usage of pseudogene templates in *IgVλ* GCV. GCV is a type of unidirectional HR that uses upstream IgV pseudogenes as template (donor) sequences. *IgVλ* has 25 pseudogenes in its upstream region. We analyzed the *IgVλ* GCV tracts of WT and *TET3*-KO cells and estimated which pseudogenes were used as GCV templates (Figure 3a,b). In *TET3*-KO cells, along with the decrease of total GCV events, the diversity in pseudogene template usage was markedly reduced (Figure 3a,b), with only three pseudogenes used as templates (ψ8, ψ11 and ψ24), whereas 14 pseudogenes (ψ3, ψ4, ψ5, ψ7, ψ8, ψ10, ψ12, ψ13, ψ14,

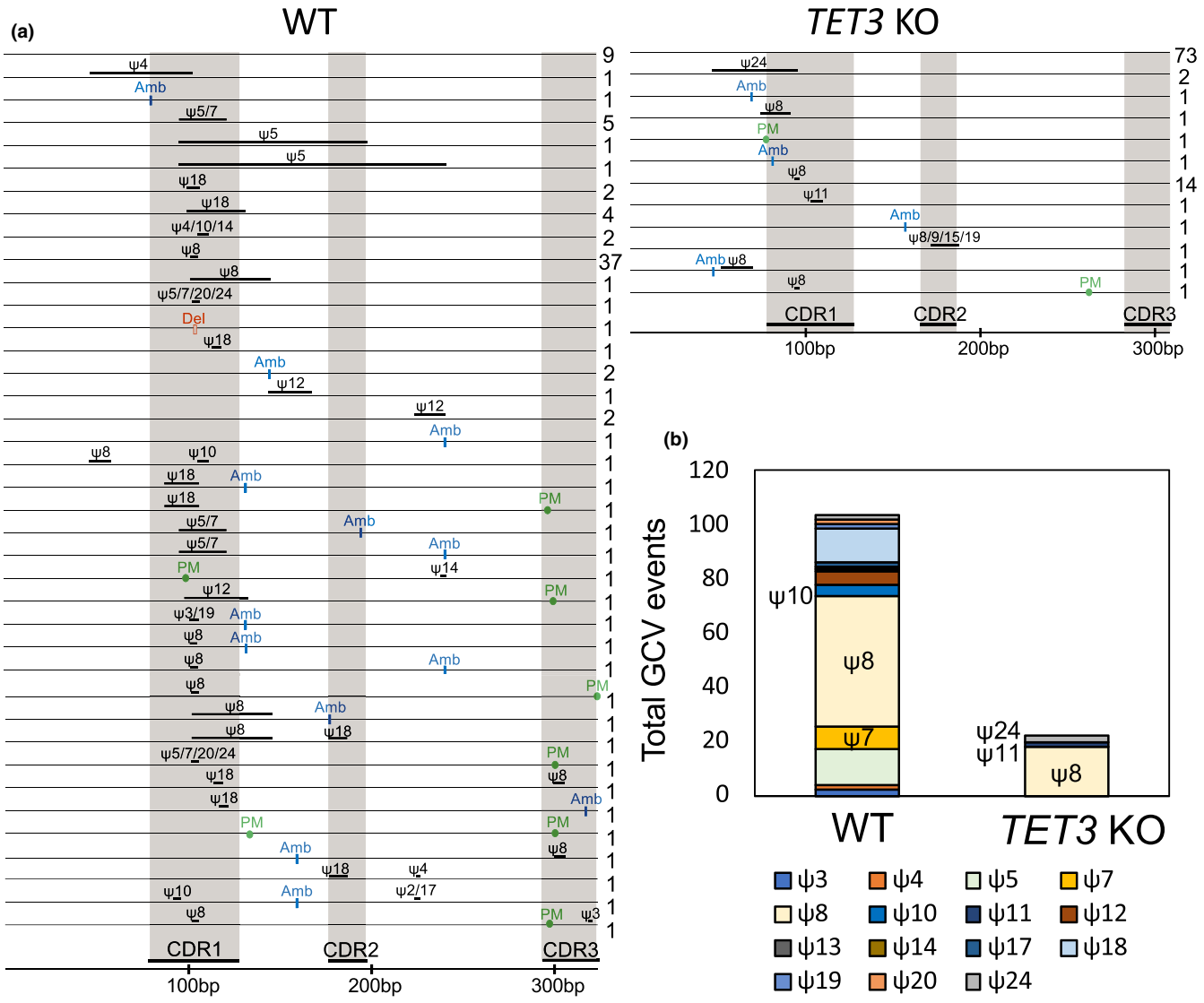

FIGURE 3 Altered usage of pseudogene templates for GCV in *TET3*-KO. (a) Identified pseudogenes used for GCV tracts in WT and *TET3*-KO cells are indicated with horizontal lines with the pseudogene numbers. Other types of mutations are also indicated above the sequences. The number of clones with each sequence pattern is given on the right side. Note that *TET3*-KO exhibited less diversity in the usage of pseudogene templates for GCV (cf. Results). (b) Usage frequency of pseudogenes in WT and *TET3*-KO cells. The number of events observed for each pseudogene was counted from the sequences analyzed in (a)

ψ17, ψ18, ψ19, ψ20 and ψ24) were employed for *IgVλ* GCV in WT. It should be noted that although the usage of ψ8 was still detectable in *TET3*-KO, its GCV frequency was severely reduced (Figure 3b).

Pseudogene ψ8 shows a higher sequence similarity to the *IgVλ* segment in DT40-CL18; hence, it is frequently used for GCV in WT DT40-CL18 cells. Consistent with previous literature (Kitao et al., 2008; Seo et al., 2005), we observed a high frequency of the usage of ψ8 (Figure 3b). However, ψ7 was also frequently employed in GCV of WT, despite a relatively lower similarity with *IgVλ* (Figure 3b). ψ10 exhibits relatively higher sequence similarity to the *IgVλ* segment in DT40-CL18, but was less utilized in GCV of WT (Figure 3b). Thus, there seems to be no clear relationship among effects of *TET3* deletion, GCV frequency in WT and sequence similarity of pseudogenes to the *IgVλ* segment, suggesting the possibility that the deletion of TET3 may have differentially affect individual pseudogenes, possibly by altering their DNA methylation status.

2.4 | Involvement of TET3 in the maintenance of low methylation at non-CpG cytosines in pseudogenes

We next assessed the effects of *TET* KOs on global levels of 5-hydroxymethylcytosine (5hmC) by dot blot analysis using anti-5hmC antibodies (Figure 4a). In contrast with *TET1*-KO and *TET2*-KO cells, which exhibited a slight increase or decrease in global 5hmC levels compared with the WT level, respectively, we observed a marked decrease in global 5hmC levels in *TET3*-KO cells. These results imply that TET3 plays a primary role to convert 5mC to 5hmC and regulate the DNA methylation levels of DT40 genomic DNA. The reason why *TET1*-KO and *TET2*-KO mutants are less affected is unknown, but it is consistent with the previous observations that each TET protein has distinct tissue-specific or cell type-specific functions (Ito et al., 2010; Rasmussen & Helin, 2016; Wu & Zhang, 2017).

To uncover the targets of TET3-mediated DNA demethylation, we performed bisulfite sequencing at several candidate loci in WT and *TET3*-KO cells (Figure 4b–e). In this study, we focused on 5 loci including 3 pseudogenes (ψ7, ψ8 and ψ10, which were employed in GCV either of WT or *TET3*-KO cells as explained in the previous section), the *IgVλ* segment and the core region of the DIVAC (diversification activator) element, downstream of *IgVλ* required for the enhancement of SHM and GCV (Blagodatski et al., 2009; Kohler et al., 2012; Kothapalli et al., 2008).

We found that the methylation index (mC/C, expressed as a percentage) in *TET3*-KO cells was significantly higher (about threefold) in pseudogenes ψ8 and ψ7 compared with WT (Figure 4b,c). DNA methylation levels at the *IgVλ* and DIVAC loci were slightly increased in *TET3*-KO cells, but remained at very low levels (2.5% and 2.0% on average, respectively).

Further in-depth analysis of the effects on DNA methylation by distinguishing between CpG sites and non-CpG sites (Figure 4d,e) revealed that DNA methylation in CpG sites was less significantly affected in *TET3*-KO cells. More importantly, the cytosines in a non-CpG context were persistently hypermethylated, particularly at all three pseudogenes in *TET3*-KO cells (Figure 4e). The methylation levels at non-CpG cytosines in pseudogenes showed stark differences from those at the *IgVλ* and DIVAC. It should be noted that most cytosines in the tested loci are in a non-CpG context (84%–90% in each target, Figure S3), meaning that the higher levels of unclassified DNA methylation in *TET3*-KO cells can be largely explained by the observed increase of DNA methylation in non-CpG cytosines. These results support the notion that TET3-mediated DNA demethylation at non-CpG cytosines in individual pseudogenes affects pseudogene usage during Ig GCV.

2.5 | TET1 and TET3 cooperatively upregulate AID expression and promote GCV

Although *TET3*-KO cells did not show a remarkable difference in the mRNA levels of GCV-associated genes (Figure 1d,e, and Figure S2), *TET1*-KO cells demonstrated a moderate but significant reduction in AID expression (Figure 1e). This result can explain the lowered sIgM gain in *TET1*-KO cells (Figure 2a,b) and suggests that TET1 may play a role in promoting AID expression. Interestingly, previous studies have shown that double *TET* deletions (*TET2/3* DKO mice) cause more detrimental effects on B cells than single *TET* deletions do (Dominguez et al., 2018; Lio et al., 2016; Orlanski et al., 2016).

We thus tested whether disruption of both TET1 and TET3 show more consequent effects on AID expression. We found that *TET1* and *TET3* double knockouts (*TET1/3* DKO cells) showed a dramatic reduction of *AID* mRNA levels (about 17% of WT levels) (Figure 5a), which was much more severe than that in single *TET1*-KO or *TET3*-KO cells, respectively (Figure 1e). To explore the potential of TET1 and TET3-mediated DNA demethylation on AID expression, we performed bisulfite sequencing at the putative promoter region of *AID* (Figure S4). While *TET1/3* DKO cells had slightly higher methylation levels than WT, the difference was not enough to account for the impaired expression of AID in *TET1/3* DKO cells. Although the underlying mechanism remains to be clarified, it is likely that TET1 and TET3 redundantly and cooperatively regulate AID expression in DT40 cells. On the other hand, *IgVλ* mRNA levels were not significantly

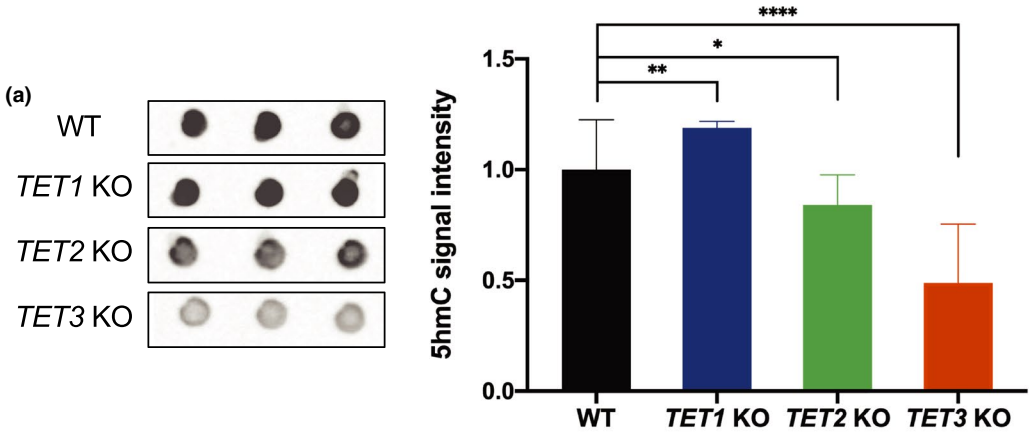
(a)
WT
TET1 KO
TET2 KO
TET3 KO
5hmC signal intensity
1.5
1.0
0.5
0.0
****
*
**
WT
TET1 KO
TET2 KO
TET3 KO

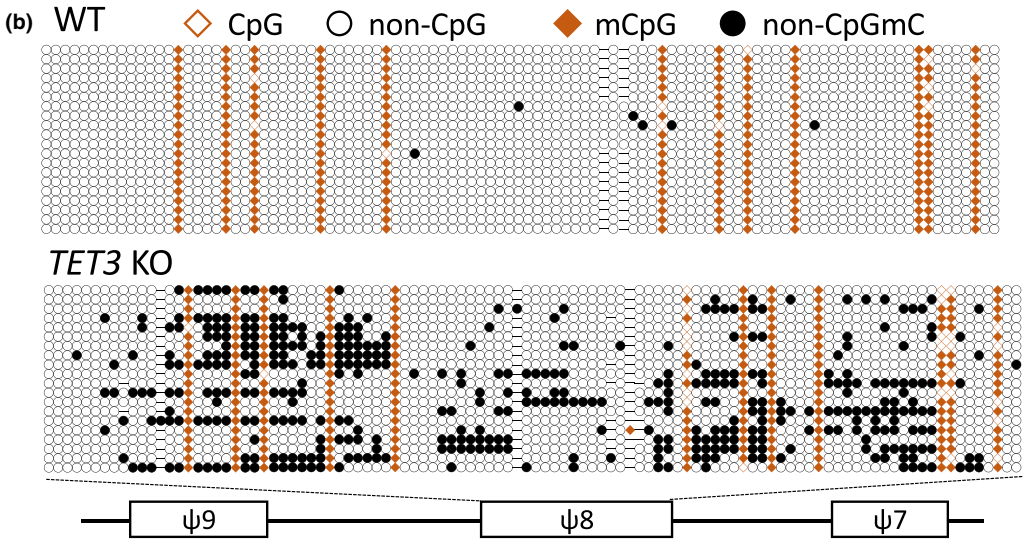
(b) WT
CpG
non-CpG
mCpG
non-CpGmC
TET3 KO
ψ9
ψ8
ψ7

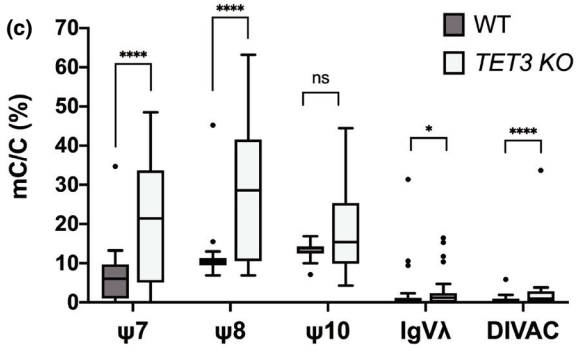
(c)
mC/C (%)
WT
TET3 KO
****
****
ns
*
****
ψ7
ψ8
ψ10
IgVλ
DIVAC

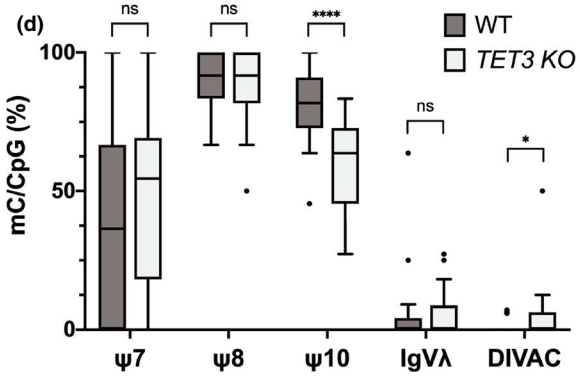
(d)
mC/CpG (%)
WT
TET3 KO
ns
ns
****
ns
*
ψ7
ψ8
ψ10
IgVλ
DIVAC

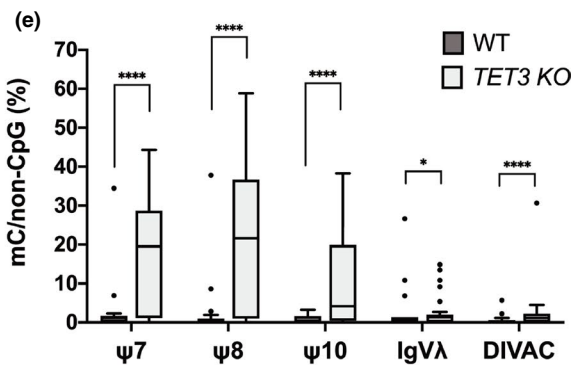
(e)
mC/non-CpG (%)
WT
TET3 KO
****
****
****
*
****
ψ7
ψ8
ψ10
IgVλ
DIVAC

FIGURE 4 TET3-dependent maintenance of genome-wide 5hmC levels and protection of pseudogenes from methylation at non-CpG sites in Ig pseudogenes. (a) Total 5hmC levels of WT, *TET1*-KO, *TET2*-KO and *TET3*-KO cells assessed by anti-5hmC dot blot. The left panel shows the dot blot results of the genomic DNA isolated from representative clones, and the quantification of them is shown in the right panel. The levels of 5hmC were normalized to the WT levels, and the thin vertical bars indicate the *SD* of triplicates (ns; not statistically significant ($p > .05$), *$p < .05$, **$p < .01$, ****$p < .0001$, unpaired *t* test with Welch's correction). (b) Representative methylation patterns of WT and *TET3*-KO cells in the pseudogene ψ8, estimated by the bisulfite-sequencing analysis. Each row represents the sequence from one clone. Here, we show 20 representative clones (out of 70) which exhibited median levels of methylation. Unmethylated or methylated cytosines are represented by open or filled marks. Black and red marks correspond to cytosines in a non-CpG context or CpG context, respectively. (c) Quantification of the methylation levels of cytosines in pseudogenes (ψ7, ψ8 and ψ10), *IgVλ* and DIVAC element from WT and *TET3*-KO cells. The ratio of methylated cytosines to all cytosines (mC/C in %) is shown. The methylation levels were calculated from the results of bisulfite sequencing. The boxes extend from the 25th to 75th percentiles of each population with Tukey whiskers (ns; not statistically significant, *$p < .05$, ****$p < .0001$, Mann–Whitney test). (d) The ratio of methylated cytosines to cytosines in a CpG context (mC/CpG in %) in the target regions. Data were obtained and analyzed as described in (c). (e) The ratio of methylated cytosines to cytosines in a non-CpG context (mC/non-CpG in %) in the target regions. Data were obtained and analyzed as described in (c)

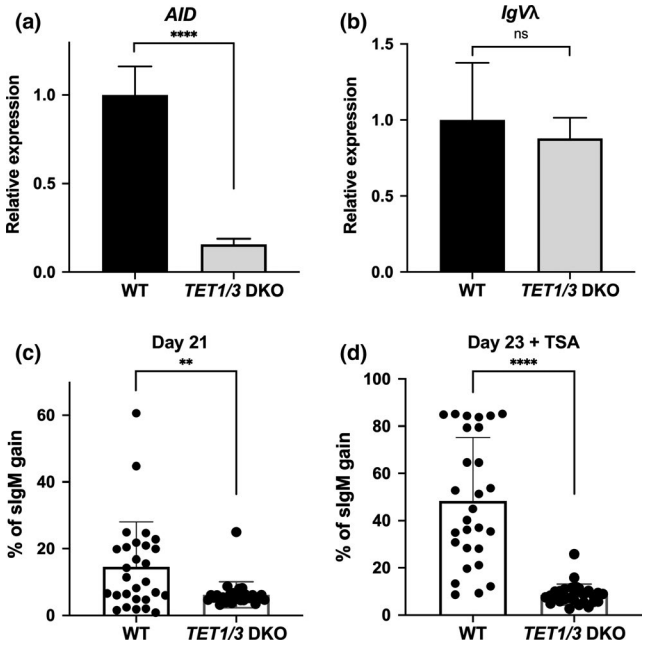

FIGURE 5 Redundant roles of TET1 and TET3 in AID expression. (a) *AID* mRNA levels in WT and *TET1/3* DKO cells quantified by RT-qPCR. The expression levels were normalized to β-actin and then to the WT levels. The thin vertical bars show the *SD* of at least four biological replicates (WT $n = 8$, for DKO $n = 4$) (ns; not statistically significant, ****$p < .0001$, unpaired *t* test with Welch's correction). (b) *IgVλ* mRNA levels in WT and *TET1/3* DKO cells quantified by RT-qPCR. The expression levels were analyzed and shown as described in (a) (WT $n = 20$, for DKO $n = 4$). (c) The sIgM gain assay of WT and *TET1/3* DKO cells. The percentage of sIgM(+) cells after 21 days of culture without TSA was determined by flow cytometry. In total, 28 subclones (shown as circles) per cell line were analyzed. The error bars indicate the *SD* of all subclone (ns; not statistically significant, **$p < .01$, ****$p < .0001$, unpaired *t* test with Welch's correction). (d) The sIgM gain assay after 23 days of culture with TSA treatment. Data were obtained and analyzed as described in (c)

affected in *TET1/3* DKO cells (Figure 5b), indicating that TET proteins do not directly contribute to the control of *IgVλ* expression in DT40 cells. We also conducted the sIgM gain assay for WT and *TET1/3* DKO cells (Figure 5c,d). Consistent with the marked decrease in AID expression, *TET1/3* DKO cells exhibited a marked loss of sIgM gain both with and without TSA treatment (Figure 5c,d). This result supports that both TET1 and TET3 are involved in the activation of AID expression and subsequent GCV in DT40 cells.

3 | DISCUSSION

We discovered that TET3 dioxygenase is involved in GCV in DT40 cells. There are at least three possibilities for the role of TET3 in Ig diversification. The first possibility is that TET3 contributes to the modulation of DNA methylation in pseudogene segments to improve the local DNA accessibility of each pseudogene used for GCV templates. The second possible mechanism for TET3 in Ig diversification is that TET3 plays a critical role in the activation of genes involved in Ig GCV and SHM, since TET proteins are important gene regulators catalyzing 5mC demethylation. The third possibility is that TET3 protein induces DNA lesions in Ig variable regions as a by-product of the DNA demethylation process. We argue these three possibilities in the following sections.

3.1 | Control of GCV template usage by TET3-mediated DNA demethylation in non-CpG context

For the first possibility, previous studies have suggested the importance of DNA accessibility across pseudogenes by showing that the induced heterochromatin state around pseudogenes impairs gene conversion while more open chromatin states accelerate it (Cummings et al., 2007, 2008). The idea of TET3-mediated modulation of pseudogenes is consistent with our observation that *TET3*-KO exhibited a pronounced reduction in the usage diversity of pseudogene templates in GCV events.

Importantly, the bisulfite sequencing conducted in this study revealed that *TET3*-KO had a marked increase in 5mC levels in some pseudogenes. In addition, the induced levels of 5mC were much higher (15%–30%) compared with those in *IgVλ* and DIVAC (less than 5%). It is thus likely that TET3 is targeted to pseudogene segments to repress local DNA methylation. A reduction in local DNA methylation is supposed to increase local DNA accessibility, so that pseudogenes with less 5mC are supposed to be preferentially utilized as Ig GCV templates.

Another finding of interest is that TET3-mediated demethylation is often found at cytosines in a non-CpG context, which was first described in the plant genome (Feng et al., 2010; Lindroth et al., 2001). In mammals, the majority of DNA methylation occurs at cytosines in a CpG context. Non-CpG comprises a very small portion of total methylated sites in differentiated somatic human cells, except for embryonic stem cells and neuronal cells (Jang et al., 2017; Ziller et al., 2011). It was reported that in chicken breast muscle tissue, genome-wide methylated CpG content among methylated cytosines is about 95% (Zhang et al., 2017). The frequency of methylated CHG or methylated CHH (where H is A, C or T) is about 1% and 4%, respectively (Zhang et al., 2017). Thus, mammalian and avian TET proteins are believed, for the most part, to catalyze demethylation of 5mCpG (Hu et al., 2013; Ravichandran et al., 2018). Our results illustrate that the increased levels of 5mC in *TET3*-KO is largely attributable to methylation at non-CpG sites rather than that at CpG sites.

The molecular mechanism of TET3-targeting to non-CpG sites in the Ig pseudogenes is unknown. Previously, however, Guo *et al*. reported that strand-specific non-CpG methylation occurs in short interspersed nuclear elements (SINEs) and long interspersed nuclear elements (LINEs) in human-induced pluripotent stem (iPS) cells (W. Guo et al., 2014). It was also reported that TET proteins bind to multiple transposable elements and regulate their expression (de la Rica et al., 2016).

To note, while the interaction of TET proteins with cytosines is largely confined to CpG sites, DNMT3A can methylate non-CpG cytosines and is involved in the establishment of non-CpG methylation (Guo, Su, et al., 2014; Ramsahoye et al., 2000). In addition, recent studies have demonstrated that genomic methylation patterns are dynamically regulated by the competitive activities of TET proteins and DNMT3 (Charlton et al., 2020; Ginno et al., 2020). These reports imply the potential role of TET proteins in regulating non-CpG methylation in repetitive sequences, most likely achieved by counteracting de novo DNMTs. Future research directions will investigate the mechanisms underlying dynamics of non-CpG methylation in repetitive sequences such as transposons, retroelements and pseudogene clusters.

3.2 | Function of TET3 and TET1 in gene regulation or cis-acting elements for Ig diversification

The second possibility is that TET3 is involved in the activation of genes for Ig GCV and SHM. Indeed, TET proteins have previously been implicated in the regulation of early embryogenesis, cell differentiation and various neuronal functions (Pastor et al., 2013; Wu & Zhang, 2017). However, the results of this study clearly indicate that this hypothesis is unlikely, since many of the central players required for GCV and SHM were mostly unchanged in *TET3*-KO cells (Figure S2).

On the other hand, it should be noted that *TET1*-KO did lead to a moderate reduction in AID expression (Figure 1e), a gene that plays critical roles in the diversification of Ig variable segments in activated B cells. Furthermore, double KO of *TET1* and *TET3* (*TET1/3* DKO) exhibited more severe reduction in AID expression (Figure 5a). The mouse *Aicda* locus encoding AID contains four transcriptional controlling regions which contains cis-acting sequences for NF-κB, C/EBP, Smad3/4, STAT6, Sp1, HoxC4 and Pax5 proteins (Zan & Casali, 2013). Lio *et al*. reported that the double knockout mouse of *Tet2* and *Tet3* results in reduction in AID expression due to increased DNA methylation in the superenhancer for AID (Lio et al., 2019). Although similar regulatory elements are not identified yet in the chicken *AID* locus, these results suggest that TET1 and TET3 redundantly and cooperatively function to upregulate AID in DT40 cells. However, TET3 per se is dispensable for *AID* activation; hence, the loss of GCV in *TET3*-KO is not simply due to the reduction in AID expression.

Previous studies demonstrated that cis-acting DIVAC elements are needed for AID targeting to Ig variable regions (Blagodatski et al., 2009; Kohler et al., 2012). The DIVAC elements reside in the region spanning from the transcription start site to 9.8kb downstream of DT40 *IgVλ*. Thus, it is plausible that TET3 is targeted to DIVAC to modulate local DNA methylation levels. Here, *TET3*-KO resulted in a slight increase of 5mC levels in DIVAC (Figure 4c). However, the induced levels of 5mC remained very low (at most 1%–2%), ruling out critical involvement of TET3 in the regulation of Ig diversification through the regulation of methylation in the DIVAC elements.

3.3 | Does TET3 induce DNA breaks in *IgVλ* segments?

The third possibility is that DNA lesions are induced in the Ig variable region as a by-product of the TET3-mediated demethylation process. TET family proteins catalyze the successive oxidation of 5mC to convert it to 5hmC, then

to 5-formylcytosine (5fC), and 5-carboxylcytosine (5caC), which are eventually removed and restored to cytosine through the action of base excision repair (BER) (Wu & Zhang, 2017). The BER pathway includes the removal of a damaged base by DNA glycosylases, leaving an abasic site which is further processed by an apurinic/apyrimidinic (AP) endonuclease. AP endonuclease finally creates a nick in the phosphodiester backbone of DNA (Krokan & Bjoras, 2013). Those DNA lesions are repaired by short- or long-patch DNA synthesis, and likely trigger other mutagenic events such as gene conversion-type recombination or error-prone repair synthesis.

It should be noted that a similar mechanism has been proposed to explain the contribution of AID cytidine deaminase to induction of SHM and GCV in the Ig variable region (Di Noia & Neuberger, 2007). Thus, it is speculated that TET3 may catalyze DNA lesions within the Ig variable regions in B cells to induce Ig GCV and SHM. If this is true, the absence of TET3 should lead to an increase in 5mC within the *IgVλ* segment. However, in *TET3*-KO cells, DNA methylation levels at the *IgVλ* only slightly increased, remaining at very low levels (at most 2%–3%) (Figure 4c). This result rules out the role of TET3 in forming recombination-activating DNA breaks in the *IgVλ* segment.

4 | EXPERIMENTAL PROCEDURES

4.1 | Cell culture

DT40 cells were cultured at 39.5°C and 5% CO_2 in IMDM supplemented with GlutaMax-1 (Thermo Fisher Scientific), 10% fetal calf serum (BioWest), 1% chicken serum (Thermo Fisher Scientific), 55 μM β-mercaptoethanol and 1% penicillin/streptomycin (Thermo Fisher Scientific) as described before (Hashimoto et al., 2016; Hashimoto et al., 2019; Seo et al., 2020). For the sIgM gain assay with TSA treatment, cells were maintained in medium containing 10 nM of trichostatin A (Fujifilm).

4.2 | Generation of TET-deficient DT40 cells

All knockout vectors for *TET1*, *TET2* and *TET3* were derived from p3LoxNeo provided by Dr. Hiroshi Arakawa and constructed as follows. The upstream and downstream regions of the DSBH domain of each *TET* gene were amplified by PCR from DT40 genomic DNA using KOD-plus DNA polymerase (Toyobo). The PCR primers for each *TET* gene were designed based on the NCBI database (*TET1*: NC_006093.3, *TET2*: NC_006091.3, *TET3*: NC_006109.3). The sequences of all PCR primers used (T1KO-1, 2, 3 and 4, T2KO-1, 2, 3 and 4, and T3KO-1, 2, 3 and 4) are provided in Table S1. The upstream or downstream PCR products for the DSBH domain of each *TET* gene were then inserted into the upstream or downstream of neomycin marker cassette in p3LoxNeo, respectively, using DNA Ligation Kit Mighty Mix (Takara Bio) or 5x In-Fusion HD Enzyme Premix (Takara Bio). The *TET1* knockout vector with *gpt* marker cassette, the *TET2* knockout vector with *hisD* or neomycin marker cassette, and the *TET3* knockout vector with *hisD* or zeocin marker cassette were also constructed as described above, using the plasmids in which the neomycin cassette of p3LoxNeo is replaced by the relevant marker cassette. Transfection of the knockout vectors into CL18 DT40 cells was performed by electroporation using Gene Pulser (550 V, 25 μF) (Bio-Rad), as previously described (Hashimoto et al., 2016; Lin et al., 2008). The transfectants were transferred to selection medium containing 1,500 μg/mL G418, 5 μl/mL mycophenolic acid and either 450 μg/mL HisD or 1,600 μg/mL zeocin, in accordance with their selection marker, dispensed into 96-well plates and cultured for about 1 week. Targeted integration of the vectors was confirmed by genomic PCR using the primers T1-1 and G-1, N-1 and T1-2, T2-1 and N-2, H-1 and T2-2, N-1 and T3-1, and H-1 and T3-1 (Table S1).

4.3 | sIgM gain assay

Subclones of each mutant were isolated by limiting dilution in 96-well plates. Colonies derived from a single cell were transferred into 24-well plates and further expanded for 5–7 days. For flow cytometric analysis, 1 x 10^6 DT40 cells were washed with FCM buffer (PBS containing 0.5% bovine serum albumin (BSA) and 2 mM EDTA) and stained with FITC-conjugated anti-chicken IgM antibody (Bethyl laboratories, A30-102F) diluted 250-fold in FCM buffer at 4°C for 15 min. After washing twice with FCM buffer, cells were resuspended in FCM buffer and analyzed by NovoCyte flow cytometer (Agilent Technologies).

4.4 | Analysis of *IgVλ* diversification

After 28 days of culturing, genomic DNA was extracted with NucleoSpin Tissue (MACHEREY-NAGEL) and the *IgVλ* region was amplified by PCR using KOD-plus DNA polymerase (Toyobo) with the primers VL-1 and 2. The purified PCR products were cloned into pBluescript II SK(−) using 5x In-Fusion HD Enzyme Premix (Takara Bio), and then Sanger sequenced with VL-seq. All primers used are listed in Table S1. Sequence alignment was performed and mutations were identified by Geneious 7.1.9 (Biomatters). Each mutation was classified as previously described (Romanello et al., 2016; Sale et al., 2001). Briefly, ≧8 bp sequences

containing more than one mutation and matching any pseudogenes was categorized as gene conversion (GCV). Any ≧8 bp sequence that matched a pseudogene but harboring a single mutation that cannot be identified as either gene conversion or point mutation was classified as ambiguous (Amb). Single base substitutions around which the 8 bp sequence did not match any pseudogenes were categorized as point mutations (PM).

4.5 | RT-qPCR analysis

Total RNA was extracted with NucleoSpin RNA (MACHEREY-NAGEL) according to the manufacturer's instructions, and reverse transcription was performed with the PrimeScript RT reagent Kit (Perfect Real Time) (Takara Bio). The obtained cDNA was subjected to qPCR with the KAPA SYBR FAST qPCR Master Mix (2X) ABI Prism (Kapa Biosystems) using the StepOnePlus System (Thermo Fisher Scientific). Primers used are listed in Table S1.

4.6 | Dot blot assay

Genomic DNA was extracted with NucleoSpin Tissue (MACHEREY-NAGEL), and the concentration was measured with the Qubit dsDNA HS Assay Kit (Thermo Fisher). DNA was denatured by boiling at 95°C for 5 min followed by snap-freezing on ice. Denatured genomic DNA (25 ng) was spotted onto a nitrocellulose membrane (Roche) and ultraviolet (UV) cross-linked by DNA-FIX (ATTO). The membrane was subsequently incubated in blocking buffer (5% skim milk in TBST (Tris buffer saline containing 0.1% Tween 20)) for 2 hr at room temperature, washed three times with TBST and then incubated overnight at 4°C with a primary antibody against 5hmC diluted 10,000-fold in blocking buffer (Active Motif, Cat # 39769). After four washes with TBST, the membrane was incubated with horseradish peroxidase (HRP)-conjugated anti-rabbit IgG diluted 10,000-fold (GE healthcare) at room temperature for 2 hr. After washing four times with TBST, the blots were developed with Amersham ECL Western Blotting Analysis System (GE Healthcare) and the enhanced chemiluminescence (ECL)-based signals were detected by ImageQuant LAS4000 mini (GE Healthcare). The signals were quantified using ImageJ software (Schneider et al., 2012).

4.7 | Bisulfite sequencing

Genomic DNA was extracted with NucleoSpin Tissue, and then, bisulfite conversion was performed using the MethylEasy Xceed Rapid DNA Bisulphite Modification Kit (Human Genetic Signatures). The target region was amplified by PCR using EpiMark Hot Start Taq DNA Polymerase (New England Biolabs) with primers p7-1 and 2, p8-1 and 2, p10-1 and 2, VLbs-1 and 2, or DIVbs-1 and 2. The PCR products were then subjected to nested PCR using KOD-plus DNA polymerase (Toyobo) with the primers p7N-1 and 2, p8N-1 and 2, p10N-1 and 2, VLbsN-1 and 2, or DIVbsN-1 and 2, respectively. The purified nested PCR products were cloned into pBluescript II SK(−) and sequenced with the M13R primer as described above (Analysis of *IgVλ* diversification). Sequence alignment and identification of 5mC were performed with Geneious 7.1.9.

4.8 | Statistical analysis

Statistical analyses were performed with GraphPad Prism 8 for macOS (GraphPad Software) and are described in the relevant figure legends.

ACKNOWLEDGMENTS

We would like to thank Dr. K. Kurosawa and S. Kondo (The University of Tokyo) for construction of the *TET1*-KO strain and *TET2*-KO strain, experimental setup of bisulfite sequencing and their technical support; Dr. K. Hashimoto (The University of Tokyo) for technical support and helpful discussion on construction of the *TET3*-KO strain, sIgM gain assay, *IgVλ* sequence analysis; A. Murayama (The University of Tokyo) for technical support on plasmid preparation and Dr. H. Arakawa (Helmholtz Zentrum München—German Research Center for Environmental Health) for the generous gift of p3loxNeo plasmid. This work was supported by a Grant-in-Aid for Basic Science (20K06598). K.O. is also supported by JST CREST Grant Number JPMJCR18S3, Japan.

ORCID

Natsuki Takamura https://orcid.org/0000-0002-2671-4971

REFERENCES

Abe, T., Branzei, D., & Hirota, K. (2018). DNA damage tolerance mechanisms revealed from the analysis of immunoglobulin v gene diversification in avian DT40 cells. *Genes*, *9*(12), 614. https://doi.org/10.3390/genes9120614

Abe, T., Ooka, M., Kawasumi, R., Miyata, K., Takata, M., Hirota, K., & Branzei, D. (2018). Warsaw breakage syndrome DDX11 helicase acts jointly with RAD17 in the repair of bulky lesions and replication through abasic sites. *Proceedings of the National Academy of Sciences of the United States of America*, *115*(33), 8412–8417. https://doi.org/10.1073/pnas.1803110115

Arakawa, H., Hauschild, J., & Buerstedde, J. M. (2002). Requirement of the activation-induced deaminase (AID) gene for immunoglobulin gene conversion. *Science*, *295*(5558), 1301–1306. https://doi.org/10.1126/science.1067308

Baba, T. W., Giroir, B. P., & Humphries, E. H. (1985). Cell lines derived from avian lymphomas exhibit two distinct phenotypes. *Virology*, *144*(1), 139–151. https://doi.org/10.1016/0042-6822(85)90312-5

Bird, A. (2002). DNA methylation patterns and epigenetic memory. *Genes and Development*, *16*(1), 6–21. https://doi.org/10.1101/gad.947102

Blagodatski, A., Batrak, V., Schmidl, S., Schoetz, U., Caldwell, R. B., Arakawa, H., & Buerstedde, J. M. (2009). A cis-acting diversification activator both necessary and sufficient for AID-mediated hypermutation. *PLoS Genetics*, *5*(1), 1–11. https://doi.org/10.1371/journal.pgen.1000332

Budzyńska, P. M., Kyläniemi, M. K., Kallonen, T., Soikkeli, A. I., Nera, K. P., Lassila, O., & Alinikula, J. (2017). Bach2 regulates AID-mediated immunoglobulin gene conversion and somatic hypermutation in DT40 B cells. *European Journal of Immunology*, *47*(6), 993–1001. https://doi.org/10.1002/eji.201646895

Buerstedde, J. M., Reynaud, C. A., Humphries, E. H., Olson, W., Ewert, D. L., & Weill, J. C. (1990). Light chain gene conversion continues at high rate in an ALV-induced cell line. *EMBO Journal*, *9*(3), 921–927. https://doi.org/10.1002/j.1460-2075.1990.tb08190.x

Cedar, H., & Bergman, Y. (2009). Linking DNA methylation and histone modification: Patterns and paradigms. *Nature Reviews Genetics*, *10*(5), 295–304. https://doi.org/10.1038/nrg2540

Charlton, J., Jung, E. J., Mattei, A. L., Bailly, N., Liao, J., Martin, E. J., Giesselmann, P., Brändl, B., Stamenova, E. K., Müller, F.-J., Kiskinis, E., Gnirke, A., Smith, Z. D., & Meissner, A. (2020). TETs compete with DNMT3 activity in pluripotent cells at thousands of methylated somatic enhancers. *Nature Genetics*, *52*(8), 819–827. https://doi.org/10.1038/s41588-020-0639-9

Cummings, W. J., Bednarski, D. W., & Maizels, N. (2008). Genetic variation stimulated by epigenetic modification. *PLoS One*, *3*(12), e4075. https://doi.org/10.1371/journal.pone.0004075

Cummings, W. J., Yabuki, M., Ordinario, E. C., Bednarski, D. W., Quay, S., & Maizels, N. (2007). Chromatin structure regulates gene conversion. *PLoS Biology*, *5*(10), 2145–2155. https://doi.org/10.1371/journal.pbio.0050246

de la Rica, L., Deniz, Ö., Cheng, K. C. L., Todd, C. D., Cruz, C., Houseley, J., & Branco, M. R. (2016). TET-dependent regulation of retrotransposable elements in mouse embryonic stem cells. *Genome Biology*, *17*(1), 1–14. https://doi.org/10.1186/s13059-016-1096-8

Delhommeau, F., Dupont, S., Valle, V. D., James, C., Trannoy, S., Massé, A., & Bernard, O. A. (2009). Mutation in TET2 in Myeloid Cancers. *New England Journal of Medicine*, *360*(22), 2289–2301. https://doi.org/10.1056/nejmoa0810069

Di Noia, J. M., & Neuberger, M. S. (2007). Molecular mechanisms of antibody somatic hypermutation. *Annual Review of Biochemistry*, *76*, 1–22. https://doi.org/10.1146/annurev.biochem.76.061705.090740

Dominguez, P. M., Ghamlouch, H., Rosikiewicz, W., Kumar, P., Béguelin, W., Fontan, L., Rivas, M. A., Pawlikowska, P., Armand, M., Mouly, E., Torres-Martin, M., Doane, A. S., Calvo Fernandez, M. T., Durant, M., Della-Valle, V., Teater, M., Cimmino, L., Droin, N., Tadros, S., … Melnick, A. M. (2018). TET2 deficiency causes germinal center hyperplasia, impairs plasma cell differentiation, and promotes b-cell lymphomagenesis. *Cancer Discovery*, *8*(12), 1633–1653. https://doi.org/10.1158/2159-8290.CD-18-0657

Esteller, M. (2007). Cancer epigenomics: DNA methylomes and histone-modification maps. *Nature Reviews Genetics*, *8*(4), 286–298. https://doi.org/10.1038/nrg2005

Feng, S., Cokus, S. J., Zhang, X., Chen, P.-Y., Bostick, M., Goll, M. G., Hetzel, J., Jain, J., Strauss, S. H., Halpern, M. E., Ukomadu, C., Sadler, K. C., Pradhan, S., Pellegrini, M., & Jacobsen, S. E. (2010). Conservation and divergence of methylation patterning in plants and animals. *Proceedings of the National Academy of Sciences of the United States of America*, *107*(19), 8689–8694. https://doi.org/10.1073/pnas.1002720107

Ginno, P. A., Gaidatzis, D., Feldmann, A., Hoerner, L., Imanci, D., Burger, L., Zilbermann, F., Peters, A. H. F. M., Edenhofer, F., Smallwood, S. A., Krebs, A. R., & Schübeler, D. (2020). A genome-scale map of DNA methylation turnover identifies site-specific dependencies of DNMT and TET activity. *Nature Communications*, *11*(1), 1–16. https://doi.org/10.1038/s41467-020-16354-x

Goll, M. G., & Bestor, T. H. (2005). Eukaryotic cytosine methyltransferases. *Annual Review of Biochemistry*, *74*, 481–514. https://doi.org/10.1146/annurev.biochem.74.010904.153721

Guo, J. U., Su, Y., Shin, J. H., Shin, J., Li, H., Xie, B., Zhong, C., Hu, S., Le, T., Fan, G., Zhu, H., Chang, Q., Gao, Y., Ming, G.-L., & Song, H. (2014). Distribution, recognition and regulation of non-CpG methylation in the adult mammalian brain. *Nature Neuroscience*, *17*(2), 215–222. https://doi.org/10.1038/nn.3607

Guo, W., Chung, W. Y., Qian, M., Pellegrini, M., & Zhang, M. Q. (2014). Characterizing the strand-specific distribution of non-CpG methylation in human pluripotent cells. *Nucleic Acids Research*, *42*(5), 3009–3016. https://doi.org/10.1093/nar/gkt1306

Hashimoto, K., Kurosawa, K., Murayama, A., Seo, H., & Ohta, K. (2016). B cell-based seamless engineering of antibody Fc domains. *PLoS One*, *11*(12), 1–22. https://doi.org/10.1371/journal.pone.0167232

Hashimoto, K., Kurosawa, K., Seo, H., & Ohta, K. (2019). Rapid chimerization of antibodies. In M. Steinitz (Ed.), *Human monoclonal antibodies. Methods in molecular biology* (Vol. *1904*, pp. 307–317). Humana Press. https://doi.org/10.1007/978-1-4939-8958-4_14

He, Y.-F., Li, B.-Z., Li, Z., Liu, P., Wang, Y., Tang, Q., Ding, J., Jia, Y., Chen, Z., Li, L., Sun, Y., Li, X., Dai, Q., Song, C.-X., Zhang, K., He, C., & Xu, G.-L. (2011). Tet-mediated formation of 5-carboxylcytosine and its excision by TDG in mammalian DNA. *Science*, *333*(6047), 1303–1307. https://doi.org/10.1126/science.1210944

Hu, L., Li, Z. E., Cheng, J., Rao, Q., Gong, W., Liu, M., Shi, Y. G., Zhu, J., Wang, P., & Xu, Y. (2013). Crystal structure of TET2-DNA complex: Insight into TET-mediated 5mC oxidation. *Cell*, *155*(7), 1545–1555. https://doi.org/10.1016/j.cell.2013.11.020

Ito, S., Dalessio, A. C., Taranova, O. V., Hong, K., Sowers, L. C., & Zhang, Y. (2010). Role of tet proteins in 5mC to 5hmC conversion, ES-cell self-renewal and inner cell mass specification. *Nature*, *466*(7310), 1129–1133. https://doi.org/10.1038/nature09303

Ito, S., Shen, L. I., Dai, Q., Wu, S. C., Collins, L. B., Swenberg, J. A., He, C., & Zhang, Y. I. (2011). Tet proteins can convert 5-methylcytosine to 5-formylcytosine and 5-carboxylcytosine. *Science*, *333*(6047), 1300–1303. https://doi.org/10.1126/science.1210597

Jaenisch, R., & Bird, A. (2003). Epigenetic regulation of gene expression: How the genome integrates intrinsic and environmental signals. *Nature Genetics*, *33*(3S), 245–254. https://doi.org/10.1038/ng1089

Jang, H. S., Shin, W. J., Lee, J. E., & Do, J. T. (2017). CpG and non-CpG methylation in epigenetic gene regulation and brain function. *Genes*, *8*(6), 2–20. https://doi.org/10.3390/genes8060148

Kitao, H., Kimura, M., Yamamoto, K., Seo, H., Namikoshi, K., Agata, Y., Ohta, K., & Takata, M. (2008). Regulation of histone H4 acetylation by transcription factor E2A in Ig gene conversion. *International Immunology*, *20*(2), 277–284. https://doi.org/10.1093/intimm/dxm140

Kohler, K. M., McDonald, J. J., Duke, J. L., Arakawa, H., Tan, S., Kleinstein, S. H., Buerstedde, J.-M., & Schatz, D. G. (2012). Identification of core DNA elements that target somatic hypermutation. *The Journal of Immunology*, *189*(11), 5314–5326. https://doi.org/10.4049/jimmunol.1202082

Kothapalli, N., Norton, D. D., & Fugmann, S. D. (2008). Cutting edge: a cis-acting DNA element targets AID-mediated sequence diversification to the chicken Ig light chain gene locus. *The Journal of Immunology*, *180*(4), 2019–2023. https://doi.org/10.4049/jimmunol.180.4.2019

Krokan, H. E., & Bjoras, M. (2013). Chapter 06: Base excision repair. *Cold Spring Harbor Perspectives in Biology*, *5*(4), a012583.

Kurosawa, K., Lin, W., & Ohta, K. (2010). Distinct roles of HDAC1 and HDAC2 in transcription and recombination at the immunoglobulin loci in the chicken B cell line DT40. *Journal of Biochemistry*, *148*(2), 201–207. https://doi.org/10.1093/jb/mvq054

Lin, W., Hashimoto, S. I., Seo, H., Shibata, T., & Ohta, K. (2008). Modulation of immunoglobulin gene conversion frequency and distribution by the histone deacetylase HDAC2 in chicken DT40. *Genes to Cells*, *13*(3), 255–268. https://doi.org/10.1111/j.1365-2443.2008.01166.x

Lindroth, A. M., Cao, X., Jackson, J. P., Zilberman, D., McCallum, C. M., Henikoff, S., & Jacobsen, S. E. (2001). Requirement of CHROMOMETHYLASE3 for maintenance of CpXpG methylation. *Science*, *292*(5524), 2077–2080. https://doi.org/10.1126/science.1059745

Lio, C. W. J., Shukla, V., Samaniego-Castruita, D., González-Avalos, E., Chakraborty, A., Yue, X., Schatz, D. G., Ay, F., & Rao, A. (2019). TET enzymes augment activation-induced deaminase (AID) expression via 5-hydroxymethylcytosine modifications at the Aicda superenhancer. *Science Immunology*, *4*(34), 1–15. https://doi.org/10.1126/sciimmunol.aau7523

Lio, C. W., Zhang, J., González-Avalos, E., Hogan, P. G., Chang, X., & Rao, A. (2016). Tet2 and Tet3 cooperate with B-lineage transcription factors to regulate DNA modification and chromatin accessibility. *eLife*, *5*(November 2016), 1–26. https://doi.org/10.7554/eLife.18290

Lister, R., Pelizzola, M., Dowen, R. H., Hawkins, R. D., Hon, G., Tonti-Filippini, J., Nery, J. R., Lee, L., Ye, Z., Ngo, Q.-M., Edsall, L., Antosiewicz-Bourget, J., Stewart, R., Ruotti, V., Millar, A. H., Thomson, J. A., Ren, B., & Ecker, J. R. (2009). Human DNA methylomes at base resolution show widespread epigenomic differences. *Nature*, *462*(7271), 315–322. https://doi.org/10.1038/nature08514

McCormack, W. T., Tjoelker, L. W., & Thompson, C. B. (1991). Avian B-cell development: Generation of an immunoglobulin repertoire by gene conversion. *Annual Review of Immunology*, *9*, 219–241. https://doi.org/10.1146/annurev.iy.09.040191.001251

Muramatsu, M., Kinoshita, K., Fagarasan, S., Yamada, S., Shinkai, Y., & Honjo, T. (2000). Class switch recombination and hypermutation require activation-induced cytidine deaminase (AID), a potential RNA editing enzyme. *Cell*, *102*(5), 553–563. https://doi.org/10.1016/S0092-8674(00)00078-7

Oestergaard, V. H., Pentzold, C., Pedersen, R. T., Iosif, S., Alpi, A., Bekker-Jensen, S., Mailand, N., & Lisby, M. (2012). RNF8 and RNF168 but not HERC2 are required for DNA damage-induced ubiquitylation in chicken DT40 cells. *DNA Repair*, *11*(11), 892–905. https://doi.org/10.1016/j.dnarep.2012.08.005

Orlanski, S., Labi, V., Reizel, Y., Spiro, A., Lichtenstein, M., Levin-Klein, R., Koralov, S. B., Skversky, Y., Rajewsky, K., Cedar, H., & Bergman, Y. (2016). Tissue-specific DNA demethylation is required for proper B-cell differentiation and function. *Proceedings of the National Academy of Sciences of the United States of America*, *113*(18), 5018–5023. https://doi.org/10.1073/pnas.1604365113

Paddock, M. N., Buelow, B. D., Takeda, S., & Scharenberg, A. M. (2010). The BRCT domain of PARP-1 is required for immunoglobulin gene conversion. *PLoS Biology*, *8*(7), e1000428. https://doi.org/10.1371/journal.pbio.1000428

Pastor, W. A., Aravind, L., & Rao, A. (2013). TETonic shift: Biological roles of TET proteins in DNA demethylation and transcription. *Nature Reviews Molecular Cell Biology*, *14*(6), 341–356. https://doi.org/10.1038/nrm3589

Patil, V., Ward, R. L., & Hesson, L. B. (2014). The evidence for functional non-CpG methylation in mammalian cells. *Epigenetics*, *9*(6), 823–828. https://doi.org/10.4161/epi.28741

Ramsahoye, B. H., Biniszkiewicz, D., Lyko, F., Clark, V., Bird, A. P., & Jaenisch, R. (2000). Non-CpG methylation is prevalent in embryonic stem cells and may be mediated by DNA methyltransferase 3a. *Proceedings of the National Academy of Sciences*, *97*(10), 5237–5242. https://doi.org/10.1073/pnas.97.10.5237

Rasmussen, K. D., & Helin, K. (2016). Role of TET enzymes in DNA methylation, development, and cancer. *Genes and Development*, *30*(7), 733–750. https://doi.org/10.1101/gad.276568.115

Ratcliffe, M. J. H. (2006). Antibodies, immunoglobulin genes and the bursa of Fabricius in chicken B cell development. *Developmental and Comparative Immunology*, *30*(1–2), 101–118. https://doi.org/10.1016/j.dci.2005.06.018

Ravichandran, M., Jurkowska, R. Z., & Jurkowski, T. P. (2018). Target specificity of mammalian DNA methylation and demethylation machinery. *Organic and Biomolecular Chemistry*, *16*(9), 1419–1435. https://doi.org/10.1039/c7ob02574b

Reynaud, C. A., Anquez, V., Dahan, A., & Weill, J. C. (1985). A single rearrangement event generates most of the chicken immunoglobulin light chain diversity. *Cell*, *40*(2), 283–291. https://doi.org/10.1016/0092-8674(85)90142-4

Reynaud, C. A., Anquez, V., Grimal, H., & Weill, J. C. (1987). A hyperconversion mechanism generates the chicken light chain preimmune repertoire. *Cell*, *48*(3), 379–388. https://doi.org/10.1016/0092-8674(87)90189-9

Reynaud, C. A., Dahan, A., Anquez, V., & Weill, J. C. (1989). Somatic hyperconversion diversifies the single VH gene of the chicken with a high incidence in the D region. *Cell*, *59*(1), 171–183. https://doi.org/10.1016/0092-8674(89)90879-9

Robertson, K. D., & Wolffe, A. P. (2000). DNA methylation in Health and Disease. *Nature Reviews Genetics*, *1*(1), 11–19. https://doi.org/10.1136/bmj.1.5388.980

Romanello, M., Schiavone, D., Frey, A., & Sale, J. E. (2016). Histone H3.3 promotes IgV gene diversification by enhancing formation of AID -accessible single-stranded DNA. *The EMBO Journal*, *35*(13), 1452–1464. https://doi.org/10.15252/embj.201693958

Sale, J. E., Calandrini, D. M., Takata, M., Takeda, S., & Neuberger, M. S. (2001). Ablation of XRCC2/3 transforms immunoglobulin V gene conversion into somatic hypermutation. *Nature*, *77*(1998), 921–926.

Schlissel, M. S. (2004). Regulation of activation and recombination of the murine Igκ locus. *Immunological Reviews*, *200*, 215–223. https://doi.org/10.1111/j.0105-2896.2004.00157.x

Schneider, C. A., Rasband, W. S., & Eliceiri, K. W. (2012). NIH Image to ImageJ: 25 years of image analysis. *Nature Methods*, *9*(7), 671–675. http://dx.doi.org/10.1038/nmeth.2089

Seo, H., Hashimoto, S.-I., Tsuchiya, K., Lin, W., Shibata, T., & Ohta, K. (2006). An ex vivo method for rapid generation of monoclonal antibodies (ADLib system). *Nature Protocols*, *1*(3), 1502–1506. https://doi.org/10.1038/nprot.2006.248

Seo, H., Masuda, H., Asagoshi, K., Uchiki, T., Kawata, S., Sasaki, G., Nakazaki, Y. (2020). Streamlined human antibody generation and optimization by exploiting designed immunoglobulin loci in a B cell line. *Cellular & Molecular Immunology*, 1–17. https://doi.org/10.1038/s41423-020-0440-9

Seo, H., Masuoka, M., Murofushi, H., Takeda, S., Shibata, T., & Ohta, K. (2005). Rapid generation of specific antibodies by enhanced homologous recombination. *Nature Biotechnology*, *23*(6), 731–735. https://doi.org/10.1038/nbt1092

Suzuki, M. M., & Bird, A. (2008). DNA methylation landscapes: Provocative insights from epigenomics. *Nature Reviews Genetics*, *9*(6), 465–476. https://doi.org/10.1038/nrg2341

Verma, N., Pan, H., Doré, L. C., Shukla, A., Li, Q. V., Pelham-Webb, B., Teijeiro, V., González, F., Krivtsov, A., Chang, C.-J., Papapetrou, E. P., He, C., Elemento, O., & Huangfu, D. (2018). TET proteins safeguard bivalent promoters from de novo methylation in human embryonic stem cells. *Nature Genetics*, *50*(1), 83–95. https://doi.org/10.1038/s41588-017-0002-y

Weber, A. R., Krawczyk, C., Robertson, A. B., Kuśnierczyk, A., Vågbø, C. B., Schuermann, D., Klungland, A., & Schär, P. (2016). Biochemical reconstitution of TET1-TDG-BER-dependent active DNA demethylation reveals a highly coordinated mechanism. *Nature Communications*, *7*(1), 10806. https://doi.org/10.1038/ncomms10806

Weissmann, S., Alpermann, T., Grossmann, V., Kowarsch, A., Nadarajah, N., Eder, C., Dicker, F., Fasan, A., Haferlach, C., Haferlach, T., Kern, W., Schnittger, S., & Kohlmann, A. (2012). Landscape of TET2 mutations in acute myeloid leukemia. *Leukemia*, *26*(5), 934–942. https://doi.org/10.1038/leu.2011.326

Wu, X., & Zhang, Y. (2017). TET-mediated active DNA demethylation: Mechanism, function and beyond. *Nature Reviews Genetics*, *18*(9), 517–534. https://doi.org/10.1038/nrg.2017.33

Xu, Y., Wu, F., Tan, L. I., Kong, L., Xiong, L., Deng, J., Barbera, A. J., Zheng, L., Zhang, H., Huang, S., Min, J., Nicholson, T., Chen, T., Xu, G., Shi, Y., Zhang, K., & Shi, Y. G. (2011). Genome-wide regulation of 5hmC, 5mC, and gene expression by Tet1 hydroxylase in mouse embryonic stem cells. *Molecular Cell*, *42*(4), 451–464. https://doi.org/10.1016/j.molcel.2011.04.005

Xu, Y., Xu, C., Kato, A., Tempel, W., Abreu, J. G., Bian, C., Hu, Y., Hu, D. I., Zhao, B., Cerovina, T., Diao, J., Wu, F., He, H. H., Cui, Q., Clark, E., Ma, C., Barbara, A., Veenstra, G. J. C., Xu, G., … Shi, Y. G. (2012). Tet3 CXXC domain and dioxygenase activity cooperatively regulate key genes for xenopus eye and neural development. *Cell*, *151*(6), 1200–1213. https://doi.org/10.1016/j.cell.2012.11.014

Yamamoto, K., Hirano, S., Ishiai, M., Morishima, K., Kitao, H., Namikoshi, K., Kimura, M., Matsushita, N., Arakawa, H., Buerstedde, J.-M., Komatsu, K., Thompson, L. H., & Takata, M. (2005). Fanconi anemia protein FANCD2 promotes immunoglobulin gene conversion and DNA repair through a mechanism related to homologous recombination. *Molecular and Cellular Biology*, *25*(1), 34–43. https://doi.org/10.1128/mcb.25.1.34-43.2005

Yang, X., Han, H., DeCarvalho, D. D., Lay, F. D., Jones, P. A., & Liang, G. (2014). Gene body methylation can alter gene expression and is a therapeutic target in cancer. *Cancer Cell*, *26*(4), 577–590. https://doi.org/10.1016/j.ccr.2014.07.028

Zan, H., & Casali, P. (2013). Regulation of Aicda expression and AID activity. *Autoimmunity*, *46*(2), 83–101. https://doi.org/10.3109/08916934.2012.749244

Zhang, M., Yan, F.-B., Li, F., Jiang, K.-R., Li, D.-H., Han, R.-L., Li, Z.-J., Jiang, R.-R., Liu, X.-J., Kang, X.-T., & Sun, G.-R. (2017). Genome-wide DNA methylation profiles reveal novel candidate genes associated with meat quality at different age stages in hens. *Scientific Reports*, *7*(February), 1–15. https://doi.org/10.1038/srep45564

Ziller, M. J., Müller, F., Liao, J., Zhang, Y., Gu, H., Bock, C., Boyle, P., Epstein, C. B., Bernstein, B. E., Lengauer, T., Gnirke, A., & Meissner, A. (2011). Genomic distribution and Inter-Sample variation of Non-CpG methylation across human cell types. *PLoS Genetics*, *7*(12), e1002389. https://doi.org/10.1371/journal.pgen.1002389

SUPPORTING INFORMATION

Additional supporting information may be found online in the Supporting Information section.

How to cite this article: Takamura N, Seo H, Ohta K. TET3 dioxygenase modulates gene conversion at the avian immunoglobulin variable region via demethylation of non-CpG sites in pseudogene templates. *Genes Cells*. 2021;26:121–135. https://doi.org/10.1111/gtc.12828